Biomech Model Mechanobiol (2012) 11:947–957
DOI 10.1007/s10237-011-0364-5

ORIGINAL PAPER

History effect and timing of force production introduced in a skeletal muscle model

Natalia Kosterina · Håkan Westerblad · Anders Eriksson

Received: 21 June 2011 / Accepted: 8 December 2011 / Published online: 23 December 2011

Abstract Skeletal muscle modelling requires a detailed description of muscular force production. We have performed a series of experiments on mouse skeletal muscles to give a basis for an improved description of the muscular force production. Our previous work introduced a force modification in isometric phases, which was based on the work performed by or on the muscle during transient-length-varying contractions. Here, state-space diagrams were used to investigate the timing aspects of the force production. These show a dominant exponential nature of the force development in isometric phases of the contractions, reached after a non-exponential phase, assumed as an activation or deactivation stage and not further analysed here. The time constants of the exponential functions describing isometric force redevelopment after length variations appear to be related to the one for an initial isometric contraction, but depending on the previous history. The timing of force production calculated from the state-space diagrams was in agreement with the generally accepted muscle properties, thereby demonstrating the reliability of the method. A macroscopic muscular model consisting of a contractile element, parallel and series elastic elements was developed. The parameters from the experiment analysis, particularly the force modification after non-isometric contractions and the time constants, were reproduced by the simulations. The relationship between time constants introduced in a mechanistic model and the measured macroscale timings is discussed.

Keywords Muscular force · Length variations · State-space diagrams · Time constant · Muscle model · Hill type · Force modification

N. Kosterina
KTH Mechanics, Royal Institute of Technology, Stockholm, Sweden

H. Westerblad
Department of Physiology and Pharmacology, Karolinska Institute, Stockholm, Sweden

A. Eriksson (✉)
KTH Mechanics, Royal Institute of Technology, Osquars backe 18, 100 44 Stockholm, Sweden
e-mail: anderi@kth.se

1 Introduction

Previous work by the authors focused on the isometric force modifications taking place after transient-length muscular contractions, commonly denoted as force depression following concentric contractions and force enhancement following eccentric contractions (Kosterina et al. 2008, 2009). These studies were based on the introduction of systematic length regimes during contraction in experiments on mouse *soleus* ('SOL') and *extensor digitorum longus* ('EDL') muscles. It was concluded that the work produced by the muscle during shortening, and on the muscle during stretch, was a good predictor for this force modification when focusing on a macroscopic description of the muscle force production, rather than on a phenomenological description of the inner mechanisms (Abbott and Aubert 1952; Marechal and Plaghki 1979; Sugi and Tsuchiya 1988; Lou et al. 1998; Schachar et al. 2004; Bagni et al. 2005; Morgan 2007). The description thus aimed at a model for numerical simulations of whole-body systems, which can consider the history effects in the force producing capacity.

For the active isometric force immediately continuing a transient-length contraction, the description of a force modification is focussed on an asymptotic, i.e. a theoretical long-term steady-state force value. This was compared with the asymptotic force for an initial isometric contraction,

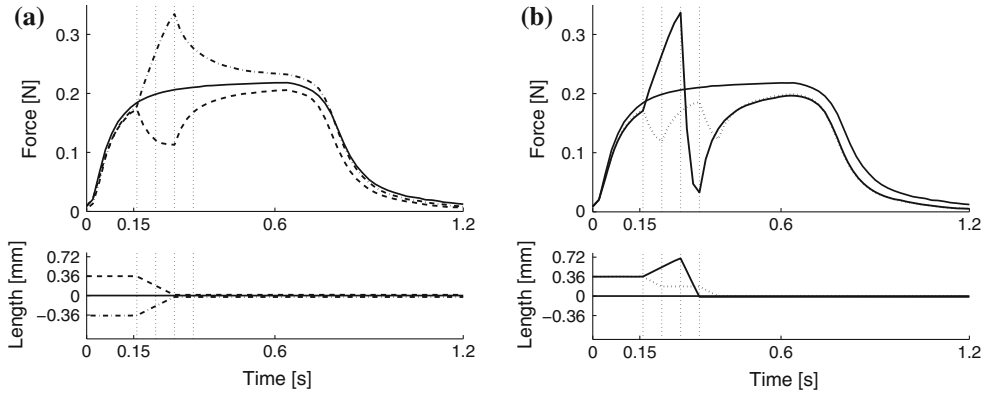

Fig. 1 Examples of force-time traces on mouse SOL muscles. *Thin solid lines* correspond to isometric contractions. Transient-length contractions: **a** *dash-dot line*—stretching and *dashed line*—shortening by 0.36 mm in 0.12 s, **b** *dotted line*—two-step shortening by 0.18 mm in 0.06 s each with 0.12-s delay between them, *thick solid line*—stretch-shortening cycle. All experiments end at the optimal length of the muscle. Time $t = 0$ denotes the stimulation start, Length $= 0$ the individual optimal length

where the same length was held constant from the start of stimulation. Such values were evaluated from the force-time trace by curve fitting (Kosterina et al. 2009). With experimental length variations according to Fig. 1, the curve fitting considered the isometric phases before and after a length variation. A good numerical fit was generally obtained with an exponential functions of the form:

$$F(t) = F_\infty + (F_a - F_\infty) \cdot \mathrm{e}^{-(t-t_a)/\tau} \tag{1}$$

where the force F at a time t goes from a value F_a at a time t_a to a steady-state asymptotic value F_∞ through an exponential function with a time constant τ (Hancock et al. 2004; Corr and Herzog 2005). The conclusion from Kosterina et al. (2008) was that the time constant τ_r for an isometric phase following shortening was—for practical purposes and on the macroscale—well predicted by the one, τ_o, for an initial isometric contraction.

The result from our previous papers, by Kosterina et al. (2008, 2009), is thereby that the transient force production in an isometric phase of a contraction following a length variation can be well predicted by the introduction of a force modification, considering the history through the work quantity, and the initial time constant, being a typical parameter for a muscle individual. The force modification, positive or negative, is here seen as a difference between the isometric forces obtainable at initial and at post-ramp isometric contractions at the corresponding length. Examples of force-time and length-time traces for one SOL muscle individual for isometric, stretch, shortening, stretch-shortening and two-steps shortening experiments are presented in Fig. 1.

Here, the further mathematical analysis of the force-time traces takes the experience from fitting Eq. (1) to isometric phases as inspiration. From a mechanical viewpoint, the contents of the equation would indicate the presence of a viscous damper in series with the force generator in the muscle. This can be seen by identifying the equation as an evolution process, where the time differential of the force is described by:

$$\dot{F}(t) \equiv \frac{\mathrm{d}F}{\mathrm{d}t} = \frac{1}{\tau}\left(F_\infty - F(t)\right) \tag{2}$$

where F_∞ is the asymptotic force, and the superposed dot denotes a time differential, i.e. the slope of the time trace. The expression emphasizes that the force value is constantly approaching the asymptotic value, in each time interval reducing the distance by the same ratio.

A common way to consider an evolution expression like the one in Eq. (2), an autonomous differential equation, is through the state-space (Thompson and Stewart 1986; Jeffrey 1990; Jordan and Smith 1999), where $F(t)$ and $\dot{F}(t)$ are seen as the axes in a plane diagram and where an expression of the form in Eq. (2) will come out as a straight line, with a slope of $-\frac{1}{\tau}$, and coming to $\dot{F} = 0$ for $F = F_\infty$. Utilization of this technique for description of the macromuscular behaviour is the main content of the present paper. We, however, would like to point to the fact that this macrotiming is phenomenologically an aggregate of several internal time constants and not immediately comparable to other time constants used in the interpolation or modelling of muscle experiments.

The state-space visualization of the experimental time-data will thus reveal if the measured quantity, here muscular force, is realistically described by a function like the one in Eq. (1). Straight lines in the diagram will confirm this assumption for a phase of the interval, whereas curved lines will correspond to phases, where either the behaviour is not exponential or the asymptotic value is not a constant attractor (Jeffrey 1990). It is already here noted that the non-isometric parts of the force-trace should not be straight lines, as the changing length will in itself implicate the differences in isometric force.

There is always a time span before the force takes the path of exponential development or redevelopment after stimulation and destimulation, respectively. These time intervals obviously correspond to some aspects of activation of the muscle, but in order to not confuse previous definitions of this term (Stephenson and Williams 1982; Stein et al. 1982), we will here use a terminology not related to internal aspects of muscle action. The present analysis thus defines periods to reach maximum and minimum (i.e. the maximal negative) rates of force-time derivative. We will denote them $t_{\triangle}$ and $t_{\triangledown}$. The time stamps of the points in the diagram indicate the different phases of behaviour. In particular, the time stamps of the end points of the straight lines in the diagram carry a meaning with respect to force-time differential extremum.

A skeletal muscle model described by Günther et al. (2007) was considered as a basis for our simulations. The model was adopted for mouse SOL and EDL muscles. A so-called history effect, emergent after active shortening and stretch (Abbott and Aubert 1952; Herzog and Leonard 1997), was introduced in the model in order to improve the numerical muscular force description. Previous attempts to include a history effect in muscle models used dependence of the force modification on ramp parameters such as amplitude and velocity, Edman (1979); Marechal and Plaghki (1979); Meijer et al. (1998). Our previous study has shown linear relationships between the force modification and mechanical work produced during stretch and shortening, Kosterina et al. (2008, 2009); this is also supported by Herzog et al. (2000); McGowan et al. (2010). The need for reasonably accurate macrolevel muscular models, considering the timing, is emphasized by studies on optimal human movements, Pettersson et al. (2010).

The present paper will discuss the analysis of muscle contraction experiments performed, by means of the state-space view, aiming at a macroscopic interpretation of the force production in the isometric phases of contractions. These findings were introduced in the rheological skeletal muscle model presented in this study. A brief review of the experiments is given in Sect. 2, which also describes the mathematical analysis procedure and the numerical muscle modelling aspects. The results are given in Sect. 3 and discussed in Sect. 4.

2 Methods

2.1 Mouse muscle experiments

The present work is built upon a set of transient-length experiments on dissected mouse SOL and EDL muscles, (Kosterina et al. 2009). The maximum admissible decrease in optimal force before discarding a specimen was set to 10%. The experiment series contained a total of 11 SOL and 14 EDL muscles. As each muscle was only used in a subset of experiments, the final results for each experiment are based on results from $n = 5 - 6$ muscles. In each experiment, the length was systematically varied during full tetanic stimulation of the muscle. The forces and the lengths were recorded for processing. Full experimental details are given in the reference, as are main characteristic data of the muscles investigated.

2.2 Data processing

Force and length data were recorded at 500 Hz during the experiments. The noise level in the data was low, hardly visible in the time traces of the quantities. As, however, for the present purposes the time differentials of the force data were needed, a filtering of the force data was performed. This filtering was defined by a second-order Butterworth lowpass recursive filter with a cut-off frequency of 60 Hz, performed in Matlab (version R2010a, The MathWorks, Inc., Natick, MA, USA). The force differential was then evaluated in the midpoints of the time steps recorded, through a central difference approximation; corresponding force values were the averages between the neighbouring points:

$$t_{i+1/2} = \frac{1}{2}\,(t_i + t_{i+1}) \tag{3}$$

$$F_{i+1/2} = \frac{1}{2}\,(F_i + F_{i+1}) \tag{4}$$

$$\dot{F}_{i+1/2} = \frac{1}{\Delta t}\,(F_{i+1} - F_i) \tag{5}$$

where the indices refer to experimental time $t_i = i \cdot \Delta t = i \cdot 0.002\,[\mathrm{s}]$ since the start of the stimulation.

2.3 State-space analysis

All the experiments were, after filtering, plotted in the state-space diagrams, with $F(t)$ as ordinate and $\dot{F}(t)$ as abscissa. The borderlines between the different isometric and isokinetic parts of the curves were marked, and each such segment treated separately. As examples, the state-space diagrams of some of the experiments are given in Figs. 2, 3, 4, and 5, with the time stamps at interesting points.

It is obvious from Figs. 2, 3, 4, and 5 that the start and end of stimulation cause non-straight lines corresponding to a preparation for isometric active and passive phases of force development and decay. In the figures, time stamps are marked where the assumed straight lines start. These points were defined as maximum and minimum values of the force-time differential, $\dot{F}(t)$, reached from the start and end of stimulation on a relevant time interval. Times $t_{\triangle}$ and $t_{\triangledown}$ for each experiment denote the intervals of this rise and drop of force rate.

When the maximum rate of force rise was reached, an exponential isometric force development began. This phase

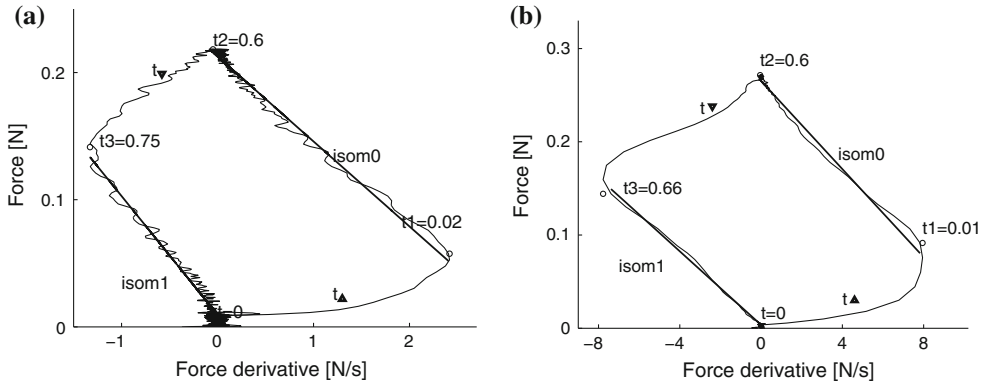

Fig. 2 State-space plot of example isometric test performed on mouse SOL (**a**) and EDL (**b**) muscles, showing the relation between current force and force-time differential values over experimental time. Time $t_0 = 0$ denotes the start of stimulation, the force-time differential, $\dot{F}(t)$, increases during $t_\triangle$ until reaching a maximum value at time t_1. Then the force, $F(t)$, rises exponentially ('isom0') and reaches a steady-state value when the $\dot{F}(t)$ drops to zero. After the stimulation terminates at time t_2, force and force derivative start to decrease. $\dot{F}(t)$ drops to its minimum value during $t_\triangledown$ (until time t_3), then the force decays exponentially to its passive level ('isom1')

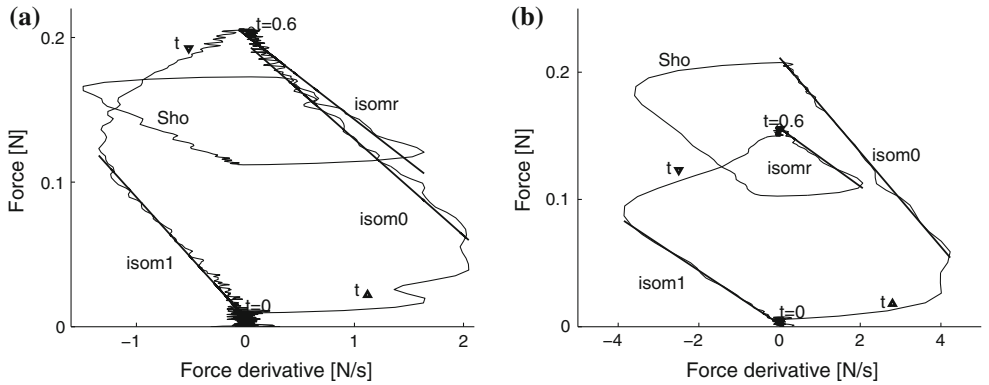

Fig. 3 State-space plot of example shortening test performed on mouse SOL (**a**) and EDL (**b**) muscles, showing the relationship between current force and force-time differential values over experimental time. Time $t = 0$ denotes the start of stimulation, and stimulation is ended at $t = 0.6$ s. The *straight lines* are regression fits of the isometric phases of muscle contractions: 'isom0'—initial force development, 'isomr'—force redevelopment after shortening, 'isom1'—force decay after destimulation. 'Sho' denotes the active shortening phase

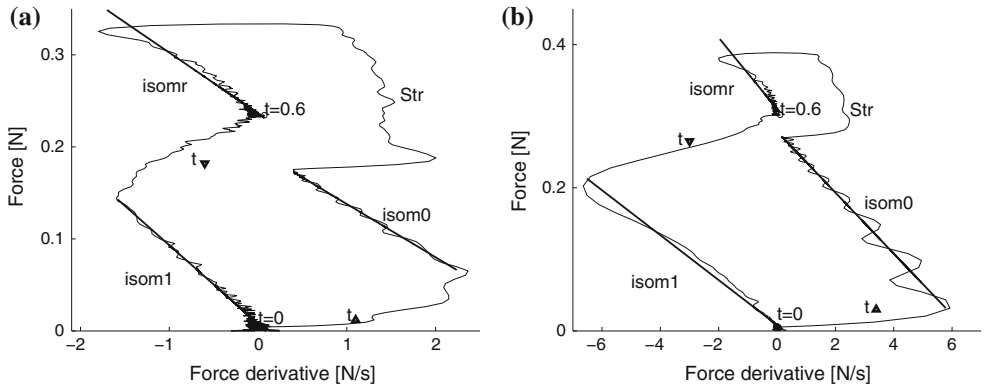

Fig. 4 State-space plot of example stretch test performed on mouse SOL (**a**) and EDL (**b**) muscles, showing the relationship between current force and force-time differential values over experimental time. Time $t = 0$ denotes the start of stimulation, stimulation is ended at $t = 0.6$ s. The *straight lines* are regression fits of the isometric phases of muscle contractions: 'isom0'—initial force development, 'isomr'—force redevelopment after stretching, 'isom1'—force decay after destimulation. 'Str' denotes the active stretch phase

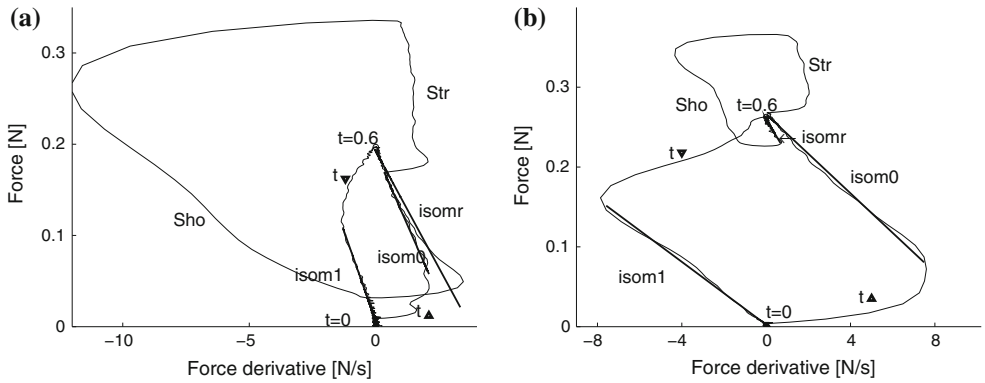

Fig. 5 State-space plot of example stretch-shortening test performed on mouse SOL (**a**) and EDL (**b**) muscles, showing the relationship between current force and force-time differential values over experimental time. Time $t = 0$ denotes the start of stimulation, and stimulation is ended at $t = 0.6$ s. The *straight lines* are regression fits of the isometric phases of muscle contractions: 'isom0'—initial force development, 'isomr'—force redevelopment after stretch-shortening ramp, 'isom1'—force decay after destimulation. 'Str' and 'Sho' denote the active stretch and shortening phases correspondingly

appeared as a straight line on the state-space diagram (Fig. 2). Change in length or activation regime leads to clear changes in the curve. A phase of force redevelopment after active lengthening or shortening was identified using time stamps, and this turned out as a straight line (Figs. 3, 4, 5). Passive force deactivation was detected using the time stamps and also appeared as a straight line.

Having defined these time instances, the time constants for the straight lines of all isometric phases can be evaluated from the straight-line fitting. The time constants can be assumed to be valid for isometric, fully active or fully passive phases. We denote by τ_0 the time constant for an active initial isometric case, by τ_r^-, τ_r^+ and $\tau_r^\pm$ the one for active recovery after shortening, stretch and stretch-shortening cycle, and by τ_1 the one for passive force loss.

As will be shown below, the time constants τ_r^-, τ_r^+ and $\tau_r^\pm$ for the active phases of the experiments are related to the initial time constant, τ_0, for a specific muscle individual.

2.4 Modelling

Simulation of muscular force generation was based on the work done by Günther et al. (2007) and van Soest and Bobbert (1993) and was implemented in Matlab. A muscle-tendon complex was represented as a contractile element (CE) in parallel with an elastic element (PEE) and connected to a series elastic element (SEE), Fig. 6. Both elastic elements contain a damping components (D_{PE}, D_{SE}) in order to avoid high-frequency oscillations that might occur in impact (Günther et al. 2007; Rode et al. 2009). In our work, force modification component (Mod) is added in parallel to both CE and SEE.

The activation dynamics of a muscle is modelled as described by Ebashi and Endo (1968) and Hatze (1977), where the isometric force F_{CE} is scaled by the activation

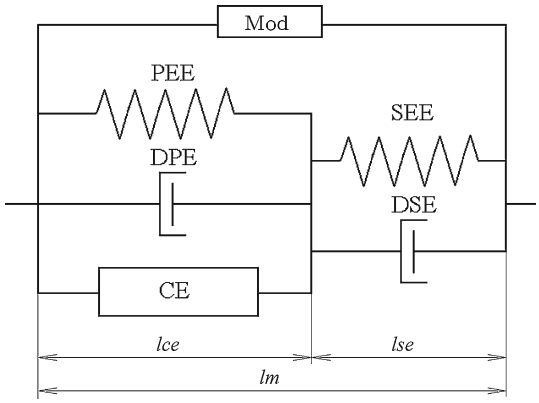

Fig. 6 Schematic representation of the muscular model. The muscle-tendon model consists of two main components: the contractile element (CE) with parallel damped elastic element (PEE, D_{PE}), both of the same length, and the serial damped elastic element (SEE, D_{SE}). In total, they form a whole muscle of length l_m, the sum of l_{CE} and l_{SE}. Force modification element (Mod) is placed parallel to CE and SE components

q, which in turn represents the Ca^{2+} concentration of the muscle, Günther et al. (2007). The muscle deactivation after stimulation termination differs from the activation dynamics; therefore, β_q coefficient was defined as a ratio of τ_0 to τ_1 (Eq. 1 in Günther et al. 2007). The force-length bell-curve fitting gave four parameters, ΔW_{asc}, ΔW_{des}, $\nu_{CE,asc}$ and $\nu_{CE,des}$, describing the isometric force as a function of CE length (Eq. 5 in Günther et al. 2007).

When stimulation and muscle length regimes are defined, contraction dynamics takes part. An equation for the contractile element velocity was derived by van Soest and Bobbert (1993)

$$\dot{l}_{CE} = \dot{l}_{CE}(l_m, l_{CE}, q) \tag{6}$$

as a function of the muscle length, CE length and activation q from the Hill equation, Hill (1938). The Hill parameters in the

Table 1 Parameters of a SOL muscle-tendon model for an adult male NMRI mouse used in the simulations

	Constants and values				Source
Individual muscle parameters	l_m (m)	F_0 (N)	τ_0 (s)	τ_1 (s)	
(typical values)	0.011	0.210	0.063	0.052	Exp
General parameters	$l_{CE} = l_{PE}$ (m)	l_{SE}	β_q	$K_{hist}(m^{-1})$	
	$0.6 \cdot l_m$	$0.4 \cdot l_m$	τ_0/τ_1	-3	Fit, Exp
Isometric force $F_{isom}(l_{CE})$	ΔW_{asc}	ΔW_{des}	$\nu_{CE,asc}$	$\nu_{CE,des}$	
	0.39	0.3	2.7	2	Exp, Fit
Contraction dynamics (concentric, eccentric)	$A_{rel,0}$	$B_{rel,0}$ (1/s)	$\mathcal{S}_{ecc}$	$\mathcal{F}_{ecc}$	
	0.1	1	2	1.8	Fit, Günther
Parallel elastic element (nonlinear), damping	$\mathcal{L}_{PEE,0}$	ν_{PEE}	$\mathcal{F}_{PEE}$	d_{PE} (Ns/m)	
	0.9	2.5	1	$6 \cdot F_0$	Günther, Fit
Series elastic element (nonlinear)	$\Delta U_{SEE,nll}$	$\Delta U_{SEE,l}$	$\Delta F_{SEE,0}$(N)		
	0.1825	0.073	$2 \cdot F_0$		Günther
Series damping (active force-dependent)	d_{SE} (Ns/m)	D_{SE}	R_{SE}		
	6	0.3	0.01		Günther

Some of the parameters kept as in Günther et al. (2007), and others were obtained from the experiments (Exp) or simulation fitting (Fit)

equation are dependent on current CE length, l_{CE}, and activation, q, as in Günther et al. (2007) and also Gordon et al. (1966); Julian and Morgan (1979); van Soest and Bobbert (1993). The concentric contractions were extrapolated into the eccentric region avoiding discontinuity on the boundary (Günther et al. 2007). The forces produced by CE with PE should be balanced with SE force. Considering damped PEE and SEE, the force equilibrium is

$$F_{CE}(l_{CE}, \dot{l}_{CE}, q) + F_{PEE}(l_{CE}) + d_{PE} * \dot{l}_{CE} = F_{SEE}(l_{SE}) + d_{SE}(F_{CE}) * \dot{l}_{SE}. \quad (7)$$

We solved the equation at each time instance by a secant method, giving the CE length velocity, $\dot{l}_{CE}$. The series and parallel elastic elements both have non-linear properties (Table 1). The series damping is force dependent, and the parallel damping is constant, scaled to the optimal force, F_0, to reflect individual parameters.

The history effect described in Kosterina et al. (2008, 2009) has been introduced in the model. Mechanical work, w, performed by and on the muscle was calculated for all transient phases from the beginning of stimulation. The force modifications evaluated were fitted with a straight line, and the history coefficient, K_{hist}, was defined as the slope of the line, seen as a parameter for the muscle individual. Negative work during stretch-shortening contractions was not taken into account for SOL muscles due to the ability of active shortening to suppress the effects from force enhancement invoked by preceding lengthening, Herzog and Leonard (2000); Lee et al. (2001). The force modification, $F_{mod} = K_{hist} \cdot w$, was in the model added to the total force from Eq. 7 (Fig. 6).

In order to adopt the model for the mouse muscles, 20 parameters had to be varied and tested. The anatomical muscle length when generating the optimal force was equated to $l_{m,0}$. The optimal force, F_0, and the rates of force development and fall, τ_0 and τ_1, were extracted from the isometric contractions, Sects. 2.2 and 2.3. These four parameters are the only individual characteristics. The remaining parameters were possible to keep invariable for SOL muscles, as model predictions were not significantly improved by modifying these. In order to achieve a good fit for EDL muscle contractions, more parameters must be varied for each specimen, but the higher variability in results leads to difficulties.

The optimal CE and SE lengths, $l_{CE,0}$ and $l_{SE,0}$, were always defined as 60 and 40% of the total length $l_{m,0}$, representing the ratio between the lengths of fibres and tendons with connective tissue.

3 Results

The time constants of isometric force redevelopment after non-isometric contractions are given in Table 2. The time constants of isometric force redeveloping, τ_r, are different from the initial timings, τ_0. But these time constants are similar inside the sets of experiments, as can be seen from the standard deviations for τ_r^-, τ_r^+ and $\tau_r^\pm$. A coefficient characterizing the type of non-isometric contraction, k, can be used to define the time constant, τ_r, of isometric force redevelopment as follows:

$$\tau_r = k \cdot \tau_0. \quad (8)$$

The multiplier k is presented in Table 2. The time constants for passive force loss, τ_1, appeared to be higher than the ones

Table 2 The time constants of isometric force redevelopment after non-isometric contractions and their ratios with the initial time constant

Experiments	SOL		EDL	
Isometric (rise)	τ_0	–	τ_0	–
	0.076 ± 0.018		0.035 ± 0.007	
Shortening	τ_r^-	τ_r^-/τ_0	τ_r^-	τ_r^-/τ_0
	0.046 ± 0.008	0.685 ± 0.112	0.027 ± 0.004	0.929 ± 0.129
Lengthening (negative)	τ_r^+	τ_r^+/τ_0	τ_r^+	τ_r^+/τ_0
	0.052 ± 0.009	0.721 ± 0.113	0.087 ± 0.014	2.342 ± 0.369
Lengthening-Shortening	$\tau_r^\pm$	$\tau_r^\pm/\tau_0$	$\tau_r^\pm$	$\tau_r^\pm/\tau_0$
	0.064 ± 0.006	0.775 ± 0.088	0.039 ± 0.005	1.086 ± 0.155
Isometric (fall)	τ_1	τ_1/τ_0	τ_1	τ_1/τ_0
	0.100 ± 0.025	1.335 ± 0.258	0.024 ± 0.003	0.709 ± 0.121

The time constants were calculated from a linear approximation of the $F(t) - \dot{F}(t)$ curve on isometric phases and averaged on all experiments in the corresponding set and for $n = 5 - 6$ SOL and $n = 5$ EDL muscles. The results are given as mean $\pm$ standard deviation, [s]

Table 3 Times of the force rate drop after stimulation termination, t_∇, following isometric and non-isometric contractions

Experiments	SOL	EDL
Isometric	0.170 ± 0.021	0.054 ± 0.006
Shortening	0.170 ± 0.014	0.132 ± 0.081
Lengthening	0.293 ± 0.059	0.138 ± 0.055
Lengthening-shortening	0.154 ± 0.020	0.066 ± 0.021

Results from $n = 5 - 6$ SOL and $n = 5$ EDL muscles are given as mean $\pm$ standard deviation, [s]

for active force development, τ_0, for SOL and lower for EDL (Table 2, the last line).

For isometric contractions, the times of pre-isometric force rate rise, $t_\triangle$, were 0.037 ± 0.012 s for SOL and 0.012 ± 0.005 s for EDL muscles. The times of pre-isometric force rate fall, t_∇, were 0.170 ± 0.021 s for SOL and 0.054 ± 0.006 s for EDL muscles. We can see that the EDL muscles are about 3 times faster than the SOL in activation and deactivation.

The stretch and shortening ramps were applied when the isometric force had almost reached a steady value. Therefore, it was possible to measure the time $t_\triangle$, for different initial muscle lengths. It has been noticed that a lengthened muscle reaches the maximum rate of rise faster than a shortened one. The time, $t_\triangle$, depends on the muscle length, Fig. 7, for both fast- and slow-twitch muscles, though this occurrence is not pronounced for EDL.

The force rate fall, t_∇, depends on the length history, Fig. 8, Table 3. For SOL muscles, this time after active shortening and stretch-shortening cycle is almost the same as after an isometric contraction, while deactivation after active stretch is twice as long. For EDL muscles, the fall of the force rate to a minimum value after an isometric contraction happens up to 3 times faster than after a non-isometric contraction.

The numerical muscle model has been described as a combination of contractile, elastic and damping elements, Siebert et al. (2008), Fig. 6. The set of equations used in the model was taken from Günther et al. (2007). Six parameters were obtained from the experimental force-time traces. Each of 20 other parameters was varied in order to fit the simulation output with the experimental data (Table 1). If variation did not improve the force prediction, the parameters were kept as in Günther et al. (2007). Simulation of the force during isometric, shortening, stretch and stretch-shortening contractions for a SOL muscle from experiments is plotted in Fig. 9.

The timing constants, τ, were obtained for the total force development, while in the model only the CE force component is described by the exponential function. The serial elastic element, which takes 40% of the muscle length, slows down isometric development of the total force, F_m, and speeds up isometric force fall. The time constant in the model was found to be approximately 40% longer than the experimental time constants for a good fit. Similar modifications were done for force fall during deactivation. The resulting fitting is shown on the force-time plots and the state-space diagrams (Figs. 9, 10). The timing constants $\tau_{0,\mathrm{sim}}$ calculated from the state-space plots for the simulated force appeared as 0.067 ± 0.012 s, and this is about 80% of the experimental values τ_0. The timing constants $\tau_{r,\mathrm{sim}}$ are between 60 and 140% of the experimental values τ_r. The best fit was reached for the concentric contractions.

4 Discussion

The study was motivated by an intention to improve the predictive capacity of available macroscopic transient muscle models such as the common Hill-type models. The main objectives were to evaluate an accurate description of the

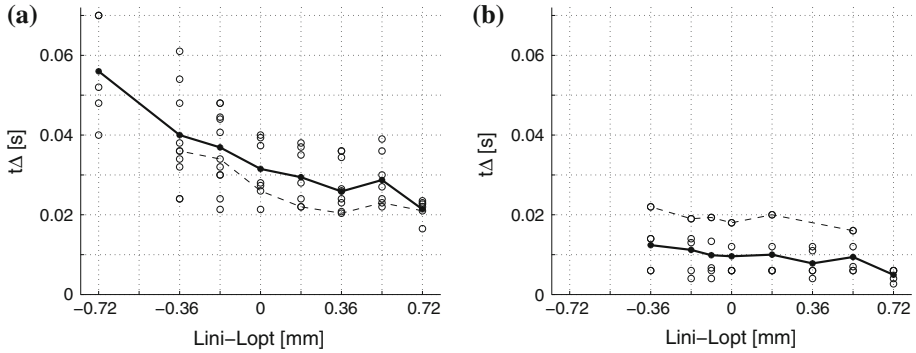

Fig. 7 Times of the force rate rise, $t_{\triangle}$, at different muscle lengths, l_{ini}, compared with optimal length, l_{opt}. The nodes of the *thick solid line* relate to a mean $t_{\triangle}$ time value of all experiments started at the corresponding length, l_{ini}, for $n = 5 - 6$ SOL (**a**) and EDL (**b**) muscles. The circles correspond to an individual muscles (mean values for isometric force development at each length), and the *dashed line* connects the individual values for a specific muscle

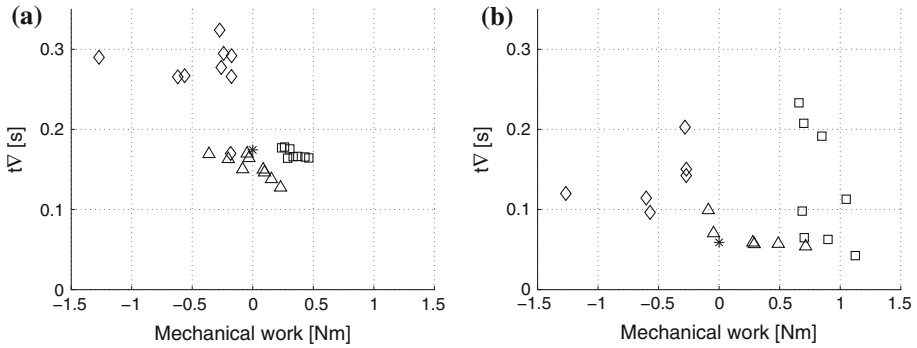

Fig. 8 Times of the force rate drop, $t_{\triangledown}$, as a function of performed mechanical work. Results from $n = 5 - 6$ SOL (**a**) and $n = 5$ EDL (**b**) muscles are presented as mean values: Shortening—*squares*, Lengthening—*diamonds*, Lengthening-Shortening—*triangles*. Average value of $t_{\triangledown}$ after an isometric contraction is marked as *asterisk*

muscular force during various regimes and to apply these findings to reproduce the muscular force generation.

To create a basis for a numerical muscle model, the timing aspects of the force production should be described. An exponential fitting of the force-time traces is generally used (Hancock et al. 2004; Corr and Herzog 2005). The state-space diagrams show linear relationships between the muscular force and the force-time differential during isometric force development. This observation confirms the admissibility of the exponential nature of the muscular force development (Stein et al. 1982), noting that the exponential phase is not reached immediately in all contexts.

The time constants characterizing the macroscopic force development at a constant muscle length were calculated from the state-space diagrams. These constants appeared approximately 2 times longer for SOL than for EDL muscles (Table 2). This is expected due to the different fibre compositions of these muscles and is consistent with previous work (Luff 1981; Ranatunga 1982; Stein et al. 1982; Brooks and Faulkner 1988).

It has been noticed that the force after non-isometric phases also follows an exponential function, Table 2. The time constants related to isometric force redevelopment following different length variations differ from the initial time constants by about 30% only. We suggest that this difference is not significant and can without major inaccuracies be neglected in a muscle model for full body modelling. This similarity makes easy the extraction of timing constant for the force recovery using the time constant of initial isometric force development. It is prominent that the time constant for the EDL muscle force redevelopment after lengthening is more than double the initial one. We assume that the slower force recovery occurs due to the vulnerability of fast muscle fibres to an active stretch, but not due to the muscle damage, since verification tests have been performed to control the isometric force level (Kosterina et al. 2009).

Passive force loss following destimulation and deactivation of the muscles can also be described by an exponential function of time (τ_1). These findings give a more accurate description of the transient muscular force variation and can be applied in the skeletal muscle model.

The state-space description allows an evaluation of times for the muscle force rate rise and fall. Here, these are defined as the times between a change in the stimulation (0/100%) and the time when the muscular force enters an exponential development curve, i.e. the straight lines in the state-space diagram. As noted above, these time intervals can be related to activation aspects of muscle, but we see them as

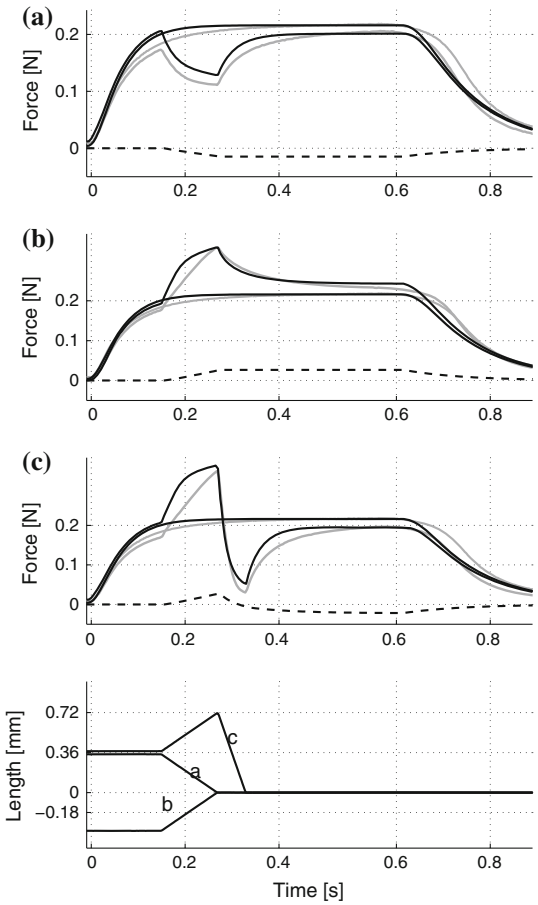

Fig. 9 Simulations (*black*) and experiments (*grey*) of non-isometric contractions: shortening (**a**), stretching (**b**) and stretch-shortening (**c**), in each case compared with isometric contraction at the final length. Force modification is plotted as *dashed line*. The length regime is plotted below the force curves. SOL muscle

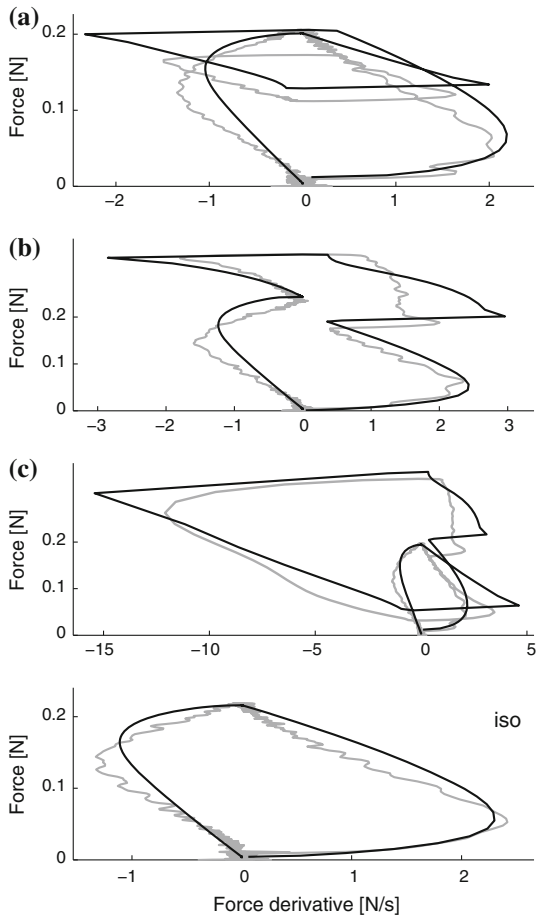

Fig. 10 Sample state-space plots of simulations of isometric contraction (iso) and non-isometric contractions: shortening (**a**), stretching (**b**) and stretch-shortening (**c**), *black lines*. Experimental values are plotted with *grey lines*. SOL muscle

mathematical constants not to be compared with previously used terms or to be related to specific internal mechanisms; however, it seems obvious that the macrotiming aspects are dependent on a set of internal events, each with its own timescale.

The $t_{\triangle}$ and $t_{\triangledown}$ times of the muscle contractions have been used as indicators of motor unit recruitment (Fang and Mortimer 1991). This is presumably based on the size principle, implying that small and slow motor units are recruited at low force levels and that gradually larger and faster motor units are recruited with the force increasing (Henneman et al. 1965; Zajac and Faden 1985). Meanwhile, Savelberg (2000) has shown that the fibre composition in a muscle also affects the rise and relaxation times, and our study confirmed this observation.

It can be noticed from Figs. 2, 3, 4, and 5 that the relationships between the force and the force-time differential after destimulation become linear after a drop of force from the steady value by approximately 50%. This validates the observation by Stein et al. (1982), who showed that the force decays exponentially after falling to a force value of one-half to two-thirds of the peak. This, in essence, also agrees with the concept of half-relaxation times, evaluated from experiments and used as a measure for de-activation timing.

Regarding the modelling part, we achieved a fairly good similarity between the experimental and the simulation traces. The timings calculated from the state-space diagrams were used to evaluate the time constants in the model, noting that the time constants are defined in different ways, depending on context, terminology and modelling assumptions. A non-isometric phase of the contractions was fairly well simulated for shortening mode and less well simulated for stretch mode due to a notable spread in the results for active lengthening and peculiarity of eccentric contractions. However, a specific mechanism of eccentric force simulation based on a recruitable elastic titin spring was proposed (Till et al. 2008; Rode et al. 2009).

An interesting observation is that the force redevelopment during the post-stretch and the post-shortening period in the muscle model can be perfectly fitted to an exponential

function, even though the total force is a solution for the equilibrium equation and is not founded upon an exponential function. Therefore, we affirm the correctness of the principal model by Günther et al. (2007) and reaffirm the relevance of Hill's equation. As we can see from Table 1, many of the parameters used by Günther et al. (2007) were kept unchanged, even though the model was used for the simulation of a different type of muscles and for another species. Many more experiments would be needed to verify the differences in these constants.

The force modification following non-isometric contractions remarkably improved the force description. Although different mechanisms are believed to cause force depression and force enhancement, these phenomena were reasonably well described by a simple formula based on the previous observations (Kosterina et al. 2009). Force modification after stretch-shortening contractions has not been thoroughly investigated yet, and a mathematical description may vary between different settings. Findings of Herzog and Leonard (2000); Lee et al. (2001) show that the effect of force enhancement disappears with the following shortening, though this contradicts another observation (Bullimore et al. 2008). The SOL and EDL mouse muscles show different force modification after stretch-shortening cycles (Kosterina et al. 2009, Fig. 3). Therefore, we did not count the negative work during stretch-shortening cycles for SOL muscles in the history-based force modification. The muscle model can be used in movement simulations, for cases where the history effect on the resulting movements is interesting.

5 Conclusions

The experimental analysis allowed us to evaluate the time constants of the exponential functions describing isometric force redevelopment after non-isometric contractions. The time constants calculated from the state-space diagrams were in agreement with generally accepted muscle properties, thereby demonstrating the reliability of the method and the presence of activation modification timing.

The numerical muscle model based on Günther et al. (2007) was adapted for SOL mouse muscles. The history effect and the timings obtained from the state-space diagrams gave better simulation results for SOL mouse muscles in a variety of length regimes.

Acknowledgments The authors gratefully acknowledge technical support in preparing muscle specimens from Shi-Jin Zhang, and financial support from the Swedish Research Council. We also thank Jan Lännergren for construction of the mechanical apparatus.

References

Abbott B, Aubert X (1952) The force exerted by active striated muscle during and after change of length. J Physiol 117:77–86

Bagni M, Cecchi G, Colombini B (2005) Crossbridge properties investigated by fast ramp stretching of activated frog muscle fibres. J Physiol 565(1):261–268

Brooks S, Faulkner J (1988) Contractile properties of skeletal muscles from young, adult and aged mice. J Physiol 404:71–82

Bullimore SR, MacIntosh BR, Herzog W (2008) Is a parallel elastic element responsible for the enhancement of steady-state muscle force following active stretch?. J Exp Biol 211: 3001–3008

Corr D, Herzog W (2005) Force recovery after activated shortening in whole skeletal muscle: Transient and steady-state aspects of force depression. J Appl Physiol 99(1):252–260

Ebashi S, Endo M (1968) Calcium ion and muscle contraction. Prog Biophys Mol Biol 18:123–166

Edman K (1979) The velocity of unloaded shortening and its relation to sarcomere length and isometric force in vertebrate muscle fibres. J Physiol 291:143–159

Fang ZP, Mortimer J (1991) A method to effect physiological recruitment order in electrically activated muscle. IEEE Trans Biomed Eng 38(2):175–179

Gordon A, Huxley A, Julian F (1966) The variation in isometric tension with sarcomere length in vertebrate muscle fibers. J Physiol 184:170–192

Günther M, Schmitt S, Wank V (2007) High-frequency oscillations as a consequence of neglected serial damping in Hill-type muscle models. Biol Cybern 97(1):63–79

Hancock W, Martin D, Huntsman L (2004) Ca^{2+} and segment length dependence of isometric force kinetics in intact ferret cardiac muscle. Circ Res 73(4):603–611

Hatze H (1977) A myocybernetic control model of skeletal muscle. Biol Cybern 25(2):103–119

Henneman E, Somjen G, Carpenter D (1965) Functional significance of cell size in spinal motoneurons. J Neurophysiol 28(3):560–580

Herzog W, Leonard T (1997) Depression of cat soleus forces following isokinetic shortening. J Biomech 30(9):865–872

Herzog W, Leonard T (2000) The history dependence of force production in mammalian skeletal muscle following stretch-shortening and shortening-stretch cycles. J Biomech 33:531–542

Herzog W, Leonard T, Wu J (2000) The relationship between force depression following shortening and mechanical work in skeletal muscle. J Biomech 33(5):659–668

Hill A (1938) The heat of shortening and the dynamic constants of muscle. Proc R Soc Lond 126:136–195

Jeffrey A (1990) Linear algebra and ordinary differential equations. Blackwell, England

Jordan D, Smith P (1999) Nonlinear ordinary differential equations: an introduction to dynamical systems, 3rd edn. Oxford University Press, New York

Julian F, Morgan D (1979) The effect on tension of non-uniform distribution of length changes applied to frog muscle fibres. J Physiol 293:379–392

Kosterina N, Westerblad H, Lännergren J, Eriksson A (2008) Muscular force production after concentric contraction. J Biomech 44(11):2422–2429

Kosterina N, Westerblad H, Eriksson A (2009) Mechanical work as predictor of force enhancement and force depression. J Biomech 42(11):1628–1634

Lee H, Herzog W, Leonard T (2001) Effects of cyclic changes in muscle length on force production in in situ cat soleus. J Biomech 34:979–987

Lou F, Curtin N, Woledge R (1998) Contraction with shortening during stimulation or during relaxation: how do the energetic costs compare?. J Muscle Res Cell Motil 19(7):797–802

Luff A (1981) Dynamic properties of the inferior rectus, extensor digitorum longus, diaphragm and soleus muscles of the mouse. J Physiol 313:161–171

Marechal G, Plaghki L (1979) The deficit of the isometric tetanic tension redeveloped after a release of frog muscle at a constant velocity. J Gen Physiol 73(4):453–467

McGowan CP, Neptune RR, Herzog W (2010) A phenomenological model and validation of shortening-induced force depression during muscle contractions. J Biomech 43(3):449–454

Meijer K, Grootenboer H, Koopman H, Van Der Linden B, Huijing P (1998) A Hill type model of rat medial gastrocnemius muscle that accounts for shortening history effects. J Biomech 31(6):555–563

Morgan D (2007) Can all residual force enhancement be explained by sarcomere non-uniformities?. J Physiol 578(2):613–615

Pettersson R, Nordmark A, Eriksson A (2010) Free-time optimization of targeted movements based on temporal FE approximation. In: Proceedings CST2010, Valencia

Ranatunga K (1982) Temperature-dependence of shortening velocity and rate of isometric tension development in rat skeletal muscle. J Physiol 329:465–483

Rode C, Siebert T, Blickhan R (2009a) Titin-induced force enhancement and force depression: a 'sticky-spring' mechanism in muscle contractions?. J Theor Biol 259(2):350–360

Rode C, Siebert T, Herzog W, Blickhan R (2009b) The effects of parallel and series elastic components on estimated active cat soleus muscle force. J Mech Med Biol 9(1):105–122

Savelberg H (2000) Rise and relaxation times of twitches and tetani in submaximally recruited, mixed muscle: a computer model. In: Herzog W (ed) Skeletal muscle mechanics: from mechanisms to function. Wiley, New York pp 225–240

Schachar R, Herzog W, Leonard T (2004) The effects of muscle stretching and shortening on isometric forces on the descending limb of the force-length relationship. J Biomech 37(6):917–926

Siebert T, Rode C, Herzog W, Till O, Blickhan R (2008) Nonlinearities make a difference: comparison of two common Hill-type models with real muscle. Biol Cybern 98:133–143

Stein R, Gordon T, Shrive J (1982) Temperature dependence of mammalian muscle contractions and ATPase activities. Biophys J 40(2):97–107

Stephenson D, Williams D (1982) Effects of sarcomere length on the force-pca relation in fast- and slow-twitch skinned muscle fibres from the rat. J Physiol 333:637–653

Sugi H, Tsuchiya T (1988) Stiffness changes during enhancement and deficit of isometric force by slow length changes in frog skeletal muscle fibres. J Physiol 407:215–229

Thompson J, Stewart H (1986) Nonlinear dynamics and chaos, 1st edn. Wiley, England

Till O, Siebert T, Rode C, Blickhan R (2008) Characterization of isovelocity extension of activated muscle: A hill-type model for eccentric contractions and a method for parameter determination. J Theor Biol 255(2):176–187

van Soest A, Bobbert M (1993) The contribution of muscle properties in the control of explosive movements. Biol Cybern 69(3):195–204

Zajac F, Faden J (1985) Relationship among recruitment order, axonal conduction velocity, and muscle-unit properties of type-identified motor units in cat plantaris muscle. J Neurophysiol 53(5):1303–1322